Structural and Multidisciplinary Optimization (2022) 65:182
https://doi.org/10.1007/s00158-022-03278-x

RESEARCH PAPER

Multi-objective optimization on diffuser of multistage centrifugal pump base on ANN-GA

Wu Tianxin[1] · Wu Denghao[1,2] · Ren Yun[3] · Song Yu[1] · Gu Yunqing[1] · Mou Jiegang[1]

Received: 19 February 2022 / Revised: 19 April 2022 / Accepted: 15 May 2022 / Published online: 15 June 2022

Abstract

As the core equipment of the water supply system, multistage centrifugal pumps produce high energy consumption every year. Thus, in the context of global warming, it is urgent to improve the efficiency of multistage centrifugal pumps. The diffuser is a key component of the pump, and it directly affects the efficiency of the pump. This research proposes a multi-objective optimization method for the diffuser based on the artificial neural network (ANN) and genetic algorithm (GA). First, diffusers are modeled parametrically by adjusting the five geometrical variables. The multi-objective optimization design of diffusers is carried out with head and Minimum Efficiency Index (MEI) as optimization objectives. MEI is an official and comprehensive index to evaluate pump efficiency under three different flow rates of $0.75Q_d$, $1.0Q_d$, and $1.1Q_d$. Meanwhile, an entropy production method is introduced as an energy loss identification tool in the proposed ANN-GA method to help evaluate the internal flow losses quantitatively and understand the root causes directly. The result shows that the multi-objective optimization method is suitable for the optimization design of diffusers under different flow rates. Compared with the original model, the head of the optimized model is improved by 1.47 m at the designed point and the C_{MEI} is reduced by 1.89. And more stable flow and lower energy loss were realized by introducing the optimized diffuser. These results provide a new solution for the optimal design of multistage centrifugal pump diffusers.

Keywords Diffuser · Multi-objective optimization · Artificial neural network · Genetic algorithm · Numerical simulation

1 Introduction

As the main energy-consuming unit, pumps consume a large number of power resources every year. Multistage centrifugal pumps are widely used in water supply systems and petrochemical industries due to their compact structure and high pressure delivery ability. The impeller as a major component of pumps directly influences pump performance, however, there are a lot of researchers have studied the optimization of impellers with different methods (Sathish et al. 2021). And the diffuser, as a major pressure conversion component of multistage centrifugal pumps, also affects the hydraulic performance of pumps largely (Zhou et al. 2012). What's more, there is still little research focusing on the optimization of diffusers. Thus, how to obtain a diffuser with better performance is still a work worthy of research.

According to previous researches, diffusers' geometry shape affects multistage pumps' performance, and every geometric parameter of diffusers affects diffusers' performance differently. Zhou et al. (2016) adjusted the trailing edge position of diffuser vanes, and they found that the extension of the trailing edge can suppress the evolution of the vortex. Wei et al. (2020) found that the vane inlet angle of the diffuser would affect the optimum operating point of the pump. Pei et al. (2020) analyzed the relationship between the wrap angle of the impeller and diffuser and pointed out that the wrap angle has a great influence on the flow in the diffuser. Wu et al. (2021) studied the performance of the diffuser with different vane numbers and pointed out that the vane number has a large effect on the performance of the pump. As mentioned above, the optimization of diffusers is a

Responsible Editor: Emilio Carlos Nelli Silva

✉ Wu Denghao
wdh@cjlu.edu.cn

[1] College of Metrology and Measurement Engineering, China Jiliang University, Hangzhou 310018, Zhejiang, China

[2] Leo Group Pump Co., Ltd, Taizhou 317511, Zhejiang, China

[3] Zhijiang College, Zhejiang University of Technology, Shaoxing 312030, Zhejiang, China

multi-factor optimization problem, and how to get a balance between different parameters needs further study.

Researchers have used a variety of methods to optimize the diffuser, and the performance of centrifugal pumps has been improved accordingly. (Si et al. 2013; Long et al. 2016; Yang et al. 2021). The traditional optimization method depends on the experience of researchers, and only with rich design experience can achieve a design with higher performance. However, this traditional method is unstable. To obtain a stable optimization method, the Design of Experiments (DOE) was applied to optimize the centrifugal pump diffuser due to its ability to reduce the number of trials. Si et al. (2013) obtained the weights of the influence of diffuser geometric parameters on the performance of the low specific speed centrifugal pump through matrix analysis and improved the efficiency of the pump by 7% under design conditions. Long et al. (2016) optimized the diffuser of the reactor coolant pump with an orthogonal test approach, and improved the head and efficiency of the pump. They pointed out that the low-velocity area of the passages far from the casing outlet may cause secondary reverse flow. Yang et al. (2021) optimized the diffuser meridian of a submersible pump by the Taguchi method, which greatly improved the efficiency of the pump under the design conditions, and pointed out that this method has obvious advantages in multi-factors optimization. However, the DOE method still has some limitations on global optimization.

With the rapid development of intelligent algorithms in recent years, researchers have started to apply this technology to the optimization of pumps due to its excellent global optimization capability (Goel et al. 2008; Wang et al. 2017; Derakhshan and Bashiri 2018; Guleren 2018; Pei et al. 2019b). Studies show that intelligent algorithms can quickly and comprehensively improve the performance of pumps. Goel et al. (2008)compared the performance of different surrogate models in predicting the hydraulic performance of the centrifugal pump. The test showed that the surrogate models such as artificial neural network (ANN) model not only have high prediction accuracy, but also can effectively reduce the time of the optimization process. Wang et al. (2017) used the response surface method and multi-island genetic algorithm (GA) to optimize the diffuser for efficiency, and the results showed that the efficiency under the design condition was improved by 8.65%. Guleren (2018) combined computational fluid dynamics (CFD) and GA to optimize the impeller and diffuser of a centrifugal pump and improved the head under the design condition. Derakhshan and Bashiri (2018) adopted the eagle strategy (ES) algorithm, and combined the advantages of different optimization algorithms to improve the head and efficiency of the pump. The result shows that the ES algorithm is beneficial to the optimal design of turbomachines. They believed that this optimization method has universal applicability. Pei et al. (2019b) adopted the optimization method combining two-layer ANN and particle swarm optimization to improve the efficiency by 0.454%, and pointed out that the optimization method could solve the nonlinear problem between performance and design variables of centrifugal pumps. Parikh et al. (2021) optimized a pump inducer using NSGA-II and CFD, and the efficiency of the pump was improved under different conditions. In summary, intelligent algorithms have great advantages in pump optimization design. Intelligent algorithms can greatly reduce the cost and time of optimization, and the optimization effect is stable with fewer limitations, meanwhile, it has little dependence on the design experiences.

Throughout the above studies, it is found that most studies mainly focus on the optimization of pumps under the design condition, and pay little attention to the performance under off-design conditions. Since 2015, the European Commission required that only multistage centrifugal pumps with a Minimum Efficiency Index (MEI) greater than 0.4 could be sold in the European Union, and MEI is determined by the efficiency under 0.75 Q_{BEP}, 1.0 Q_{BEP} (best efficiency point) and 1.1 Q_{BEP} (Carravetta et al. 2017). Therefore, to obtain a higher MEI value and make the product more energy efficient and competitive, the performance under various conditions needs to be considered comprehensively.

To explore whether the optimization method base on intelligent algorithms is suitable for diffusers of the multistage centrifugal pump, in this research the optimization method combining ANN and GA is used to optimize the head and MEI of a vertical multistage centrifugal pump. ANN is used to predict the performance of the pump with different diffusers, and GA is used to find the optimal model. At the same time, the influence mechanism of diffuser geometric parameters on pump performance was revealed by analyzing the flow characteristics in the pump.

2 Pump model and numerical simulation

2.1 Geometry of pump

A mature pump with high performance from pump manufacture was selected to be the baseline pump, and the multistage centrifugal pumps are composed of impellers, diffusers, chambers, and other components. Figure 1 shows the cross-section of the investigated pump. The three-stage model was adopted in this study because it can well reflect the flow characteristics in the multistage centrifugal pump and take fewer calculation resources (Stel et al. 2015). The main geometric parameters of the original impeller and diffuser are shown in Table 1. The designed parameters of the pump are as follows: the flow rate (Q_d) is 30m^3/h, the head (H_d) is 45 m, and the efficiency (η_d) is 75%.

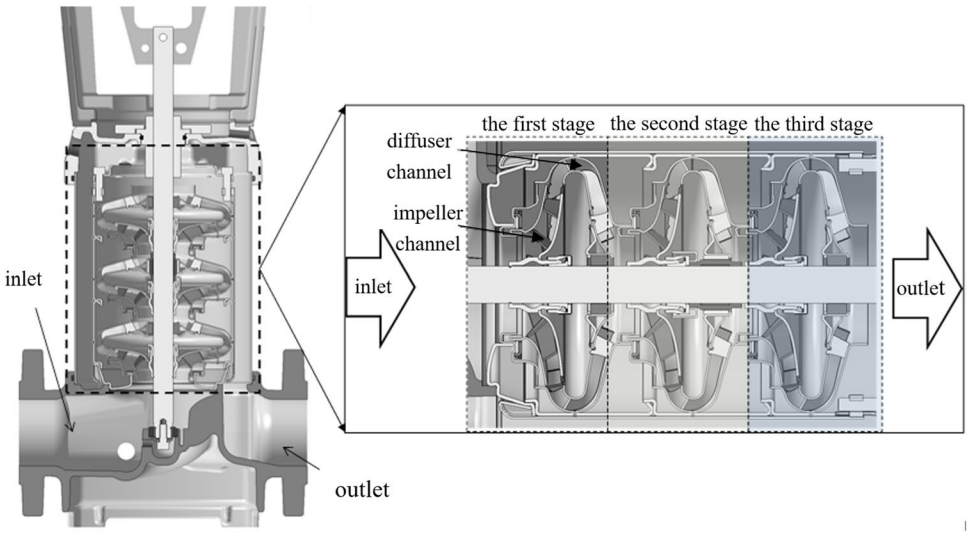

Fig. 1 Cross-section of the investigated pump

Table 1 Geometric parameters of the original impeller and diffuser

Parameters of impeller	Value	Parameters of diffuser	Value
Inlet diameter D_1	60.5 mm	Inlet diameter D_3	121 mm
Outlet diameter D_2	116 mm	Outlet diameter D_4	69 mm
Blade thickness e_1	1 mm	Blade thickness e_2	1 mm
Inlet blade angle β_1	30°	Inlet angle β_3	15°
Outlet blade angle β_2	28°	Outlet angle β_4	90°
Blade wrap angle φ_1	105°	Vane wrap angle φ_2	60.5°
Number of blades Z_1	7	Number of vanes Z_2	10

2.2 Numerical simulation

The three-dimensional, steady, incompressible Reynolds-averaged Navier–Stokes (RANS) equations are solved by ANSYS CFX to perform CFD simulations. The continuity and momentum equations are as follows (Wilcox 2006; Blazek 2015):

$$\frac{\partial u_j}{\partial x_j} = 0 \tag{1}$$

$$u_j \frac{\partial u_i}{\partial x_j} = -\frac{1}{\rho}\frac{\partial p}{\partial x_i} + \upsilon_t \frac{\partial^2 u_i}{\partial x_j \partial x_j} + \frac{1}{\rho}\frac{\partial\left(-\rho\overline{u_i' u_j'}\right)}{\partial x_j} \tag{2}$$

where u is the velocity of the flow, ρ is the density of the fluid, p is the static pressure, and ν_t is the kinematic viscosity.

According to the pre-verification, the simulation using the steady method has higher accuracy than that using the unsteady method. And steady calculation method costs fewer computing resources and time. SST k–ω turbulence model was selected for the simulations, because of its great performance in anticipating flow separation compared with the stand k–ω and k–ε models (Ren et al. 2018).

The computational domain refers to the entire flow domain within the pump, including three impellers, three diffusers, two chambers, and the pipe of inlet and outlet. The length of the inlet and outlet pipeline is set as 10 times the diameter of the inlet and outlet to improve the stability of the flow. The average $y+$ of impeller blades is 4.33, the maximum $y+$ is 13.61; the average $y+$ of diffuser vanes is 4.07, the maximum $y+$ is 8.55, and the fluid domain and mesh of the model are shown in Fig. 2. The impeller was set as rotating, and other domains were set as stationary. The frozen rotor model was set as the rotor–stator interfaces, such as the "impeller-diffuser" interface. The inlet boundary was set as the total pressure inlet with a reference pressure of 0 Pa, and the outlet boundary was set as the mass flow rate outlet. All the wetted surfaces were defined as smooth and no-slip walls. And the convergence criterion RMS (root mean square) was set as 10^{-5}.

The number of grids can affect the accuracy of numerical simulation (Yang et al. 2011). If the number of grids is too small, the error of numerical simulation results is larger, while if the number of grids is too large, it occupies more computing resources. Therefore, it is necessary to determine an appropriate number of grids. Since MEI of all models is equal to 0.7, C_{MEI} is used instead of MEI for comparison (see Sect. 3.2 for calculation of MEI). The results of the grid independence analysis are shown in Table 2. As shown in the table, the model with 6.4 million grids has a good performance, and it needs fewer computing resources. Thus, the model with 6.4 million grids is a suitable choice. Furthermore, the grid convergence index (GCI) method is used to analyze the computational convergence (Roache 1994, 1997). Table 3 presents the parameters of GCI, and a safety factor ($F_s = 1.25$) was used in the calculation of GCI_{12}

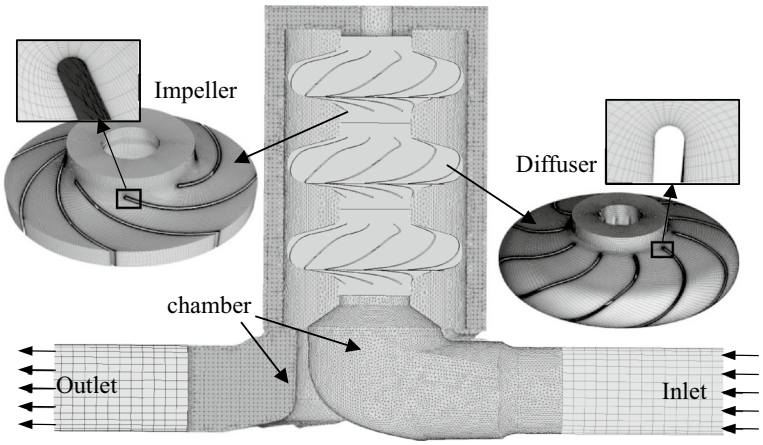

Fig. 2 The flow domain and mesh of the computational model

Table 2 The grid independence analysis

No.	Number of grids ($/10^6$)	H_i(m)	$\Delta H = \lvert H_i - H_1 \rvert / H_1$(%)	C_{MEIi}	$\Delta C_{MEI} = \lvert C_{MEIi} - C_{MEI1} \rvert / C_{MEI1}$(%)
1	12.8	45.98	0	124.20	0
2	6.4	45.51	1.02	124.58	0.31
3	3.2	44.75	2.68	125.13	0.75

Table 3 The grid convergence index

Performance (f)	Order of convergence (p)	Asymptotic solution ($f_{h=0}$)	GCI_{12} (%)	GCI_{23} (%)	$GCI_{12}/r^p GCI_{23}$(%)
H_d (m)	2.085	46.742	2.064	3.376	1.010
C_{MEI}	1.577	123.324	0.878	1.260	0.997

and GCI_{23}. Based on the result, the head is estimated to be 46.742 with an error band of 2.064%, the C_{MEI} is estimated to be 123.324 with an error band of 0.878%.

2.3 Experimental validation

To verify the accuracy of the numerical simulation, we carried out the hydraulic performance test of the prototype pump on a closed-loop testbed, as shown in Fig. 3. The accuracies of the experimental apparatus are as follows: the accuracy of the electromagnetic flowmeter ($E+H$) is 0.2%; the accuracy of the pressure transducer ($E+H$) is 0.05%; the accuracy of the torque transducer (HBM) is 0.5%. As shown in Fig. 4, the numerical simulation results are consistent with the experimental results. The average error of the head is 1.23%, the maximum error is 3.78%, and the error is relatively large under part-load conditions. The average error of efficiency is 1.89%, and the maximum error is 3.76%. However, the error of efficiency is increased under over-load conditions. In summary, the error of head and efficiency is less than 2.5% at $0.75Q_d$, $1.0Q_d$, and $1.1Q_d$, and the error of MEI is 0.70%. Therefore, it is reliable to use numerical simulation instead of the experiment to obtain pump performance.

Fig. 3 Pump test facility

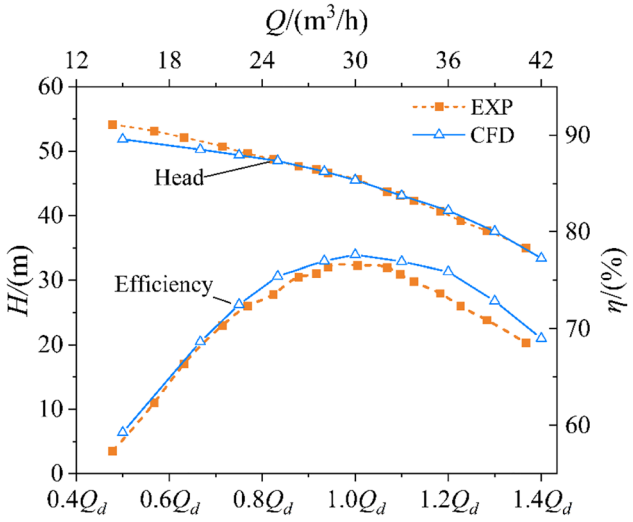

Fig. 4 Comparison of experimental and CFD results

3 Optimization

In this research, an optimization method combining ANN and GA is used to optimize the diffuser of the multistage centrifugal pump. ANN is used as the replacement of CFD to predict the performance of the pump, and GA is used to find the optimization model within the specified range. The process of optimization was shown in Fig. 5. The first step involves sampling the optimization variables using the Latin hypercube sampling (LHS) method. The next step is to create 3D models and evaluate the hydraulic performance of models by CFD. The third step is to build and train the ANN prediction model. Finally, the optimized model is found by using GA and ANN.

3.1 Optimization variables

Figure 6 shows the geometric parameters of diffusers, D_3 is inlet diameter, D_4 is outlet diameter (subscript S and H means shroud and hub respectively), D_{max} is the maximum diameter of diffusers, L_1 is axial length, L_2 is trailing edge position of vanes, β_3 is inlet angle ($\beta_3=\beta_{3S}=\beta_{3H}-0.7°$), β_4 is outlet angle, φ_2 is vane wrap angle ($\varphi_2=\varphi_{2H}=\varphi_{2S}-11.7°$), R_{in} is inlet radius of vanes, R_{out} is outlet radius of vanes.

The geometrical parameters of the diffuser directly affect the hydraulic performance of the multistage centrifugal pump, among which, axial length L_1, the trailing edge position of vane L_2, vane wrap angle φ_2, inlet angle β_3, and the number of vanes Z_2 have a great influence on the performance of the pump. Therefore, these five parameters

Fig. 5 Process of optimization

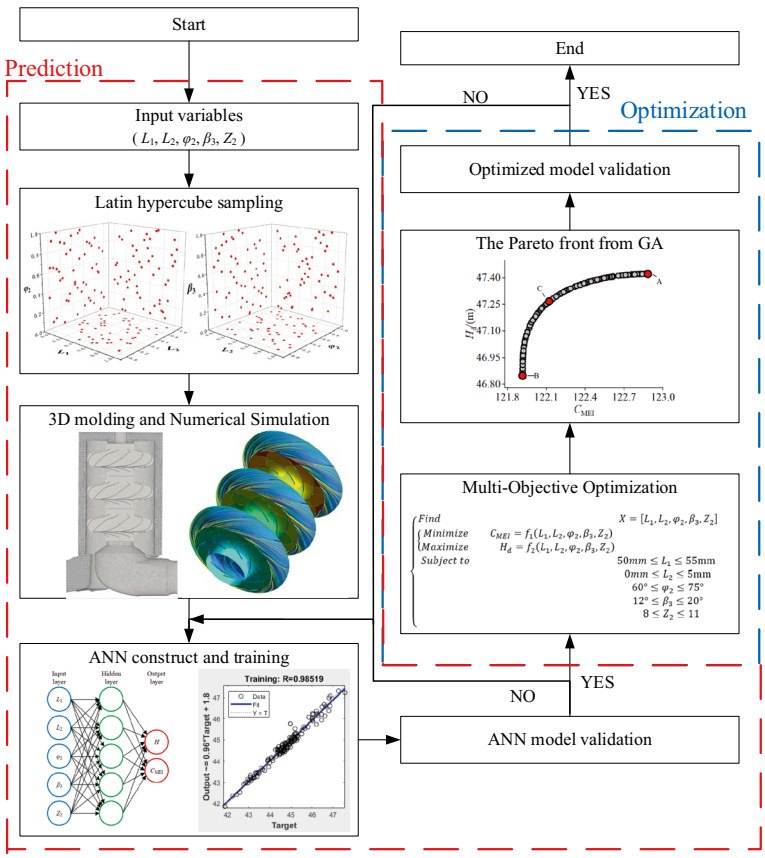

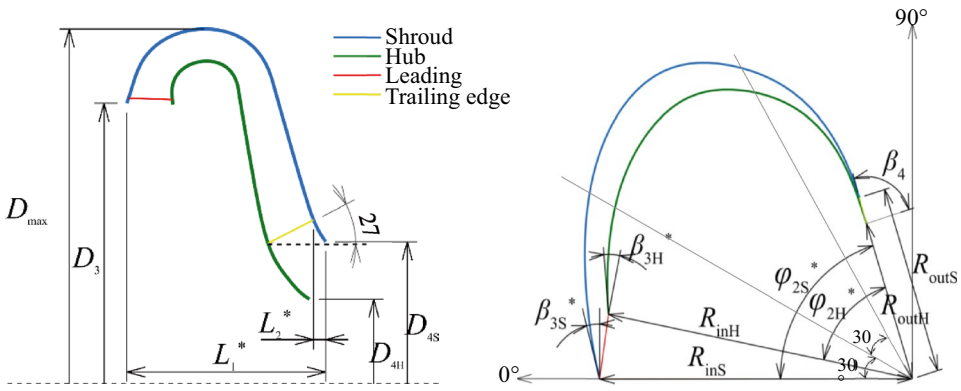

(a) Meridional shape of diffusers (b) Shape of vanes

Fig. 6 Geometric parameters of diffusers

Table 4 Range of variables

No.	Parameters of variables	Lower limit	Baseline	Upper limit
A	Axial length L_1/mm	50	52	55
B	Trailing edge position of vane L_2/mm	0	2.5	5
C	Vane wrap angle φ_2/°	60	60.5	75
D	Inlet angle β_3/°	12	15	20
E	Number of vanes Z_2	8	10	11

are selected as optimization variables in this research and marked by "*" in Fig. 6. All input parameters are the same at all pump stages. Table 4 shows the selected variables and their ranges. The variables' range had been carefully selected based on the limits of the pump structure and previous studies. A large wrap angle φ_2 can help to improve pump performance (Liu et al. 2020), so a high upper limit and a lower limit near the baseline are adopted for the range of φ_2. According to the pump structure and pre-studies, the other four variables are centered on the baseline, with a certain degree of increase or decrease as the range of their variables.

For better optimization effect, samples should cover the entire range to the greatest extent. LHS is widely used because of its great space-filling and nonlinear filling ability (McKay et al. 2000). In this research, 50 models were randomly selected from the four variables (L_1, L_2, φ_2, β_3) by the LHS method, and 200 models were obtained by setting the number of vanes Z_2 of the 50 models to 8, 9, 10 and 11, respectively.

3.2 Optimization objectives

The maximum of MEI and H_d were specified to be the optimization objectives in this research.

H_d is the head of the pump under the designed condition, it can be calculated in Eq. (3).

$$\mathrm{H_d} = \frac{P_2 - P_1}{\rho g} + \frac{v_2^2 - v_1^2}{2g} + z_2 - z_1 \tag{3}$$

where P_1, P_2 are the static pressure of the inlet and outlet liquid of the pump; v_1, v_2 are the velocity of the liquid at the inlet and outlet of the pump, z_1, z_2 are the height of the inlet and outlet.

MEI is a dimensionless scale unit of hydraulic efficiency. The calculation of MEI is based on the efficiency under the best efficiency point (BEP) $1.0Q_{BEP}$, part-load condition (PL) $0.75Q_{BEP}$, and overload condition (OL) $1.1Q_{BEP}$. It can be calculated in Eqs. (4)–(9).

F_η is an auxiliary function to calculate C_{BEP}, C_{PL}, and C_{OL}.

$$F_\eta = -11.48x^2 - 0.85y^2 - 0.38xy + 88.59x + 13.46y \tag{4}$$

where $x = \ln(n_s)$; n_s is the specific speed; $y = ln\ (Q_{BEP})$.

$$C_{BEP} = F_\eta - \eta_{BEP} \tag{5}$$

$$C_{PL} = F_\eta - \left(\frac{\eta_{PL}}{0.947}\right) \tag{6}$$

$$C_{OL} = F_\eta - \left(\frac{\eta_{OL}}{0.985}\right) \tag{7}$$

C_{MEI} is equal to the greatest of C_{BEP}, C_{PL}, and C_{OL}, as Eq. (8).

$$C_{\mathrm{MEI}} = \max\left(C_{\mathrm{BEP}},\ C_{\mathrm{PL}},\ C_{\mathrm{OL}}\right) \tag{8}$$

The value of MEI corresponding to C_{MEI} is calculated by linear interpolation between the neighboring values [as Eq. (9) and Table 5].

$$\mathrm{MEI} = 0.1\frac{C_{\mathrm{MEI}} - C_{\mathrm{left}}}{C_{\mathrm{right}} - C_{\mathrm{left}}} + \mathrm{MEI_{left}} \tag{9}$$

According to the numerical simulation results, MEI values of all the calculated models are equal to 0.7. To further study

Table 5 MEI and its corresponding C_{MEI}

MEI	C_{MEI}	*MEI*	C_{MEI}
0.1	138.19	0.5	133.43
0.2	135.41	0.6	131.87
0.3	134.89	0.7	130.37
0.4	133.95		

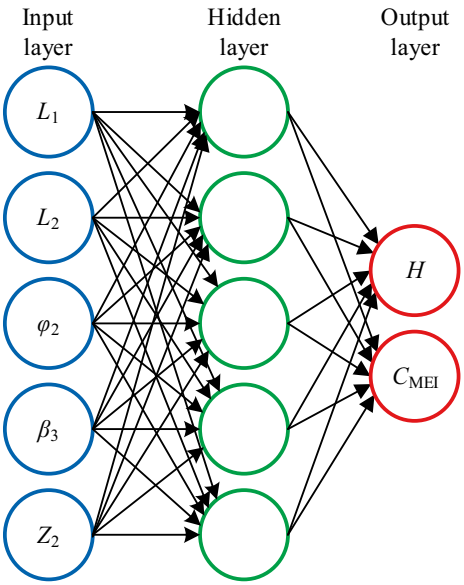

Fig. 7 The structure of BPNN

the efficiency of models, C_{MEI} is used to replace MEI as the optimization objective. The higher MEI means the smaller C_{MEI}.

3.3 Artificial neural network

Artificial neural network is widely used in industrial production due to its adaptability features integrated with the industrial problem (Meireles et al. 2003), and it has powerful nonlinear and multi-factor function fitting ability. The relationship between the geometrical parameters of the pump and hydraulic performance is highly nonlinear. The powerful function fitting ability of ANN is suitable for pump performance prediction. Back propagation neural network (BPNN) has been quite mature in theory and application. Its outstanding advantage is that it has a strong nonlinear mapping ability and flexible network structure(Han et al. 2020). Therefore, BPNN was used to predict the performance of the pump in this research. As shown in Fig. 7, the BPNN with five inputs and two outputs is adopted, which consists of one input layer, one hidden layer, and one output layer. The activation functions of the hidden layer and the output layer are tanh and linear functions, respectively. The circles represent neurons, which are the computing cells of the BPNN (as Eq. 10). The arrows show the connections between neurons.

$$y = g\left(\sum_i w_i x_i + b\right) \tag{10}$$

where w is weight, b is bias, g is activation function, x and y are input and output of neurons.

The training of BPNN is to minimize the error between the predicted value and the real value by constantly adjusting w and b. 200 samples were imported into the BPNN for training, among which 70% (140 samples) were used as the training set, 15% (30 samples) as the verification set, and 15% (30 samples) as the test set. The Levenberg–Marquardt algorithm was used as the training algorithm because its calculated mean square error is lower than other algorithms (Pei et al. 2019b).

Finally, the functions of C_{MEI} and H_d are obtained as follows:$C_{MEI} = f_1(L_1, L_2, \varphi_2, \beta_3, Z_2)$,$H_d = f_2(L_1, L_2, \varphi_2, \beta_3, Z_2)$.

3.4 Multi-objective optimization

Multi-objective optimization is often accompanied by conflicts between objectives during the optimization process, so it is difficult to obtain a unique optimization solution (Cui et al. 2017). This means we should make a balance among objectives.

In this research, the optimization objectives are the maximum of MEI (the minimum of C_{MEI}) and the maximum of H_d. The optimization variables are axial length L_1, trailing edge position of vane L_2, vane wrap angle φ_2, inlet angle β_3, and the number of vanes Z_2. This problem can be defined in Eq. (11).

As mentioned above, it is almost impossible to obtain a unique solution for the optimization design of the pump, so the conflict between objectives needs to be balanced. Pareto optimality represents an ideal state of allocation between objectives, and the Pareto Front is a set of all Pareto optimality (Pei et al. 2019a), from which can select the solution that meets requirements.

GA is used to obtain the Pareto Front here. GA is an optimization method that simulates the natural evolution process to search for solutions, and when handling complex combinatorial optimization problems, it can obtain a solution quickly. Non-dominated Sorting Genetic Algorithm-II (NSGA-II) is an improved multi-objective Genetic Algorithm, which is one of the most popular genetic algorithms at present (Deb et al. 2002). The core idea of this method is to combine a fast non-dominated sorting algorithm with elitism theory. (Sayyaadi and Babaelahi 2011). Compared with the traditional GA, it has the advantages of fast speed and good convergence. In this research, NSGA-II was used for multi-objective optimization of C_{MEI} and H_d.

$$\begin{cases} \text{Find} \quad X=[L_1, L_2, \varphi_2, \beta_3, Z_2] \\ \begin{cases} \text{minimize} \quad C_{MEI} = f_1(L_1, L_2, \varphi_2, \beta_3, Z_2) \\ \text{maximize} \quad H_d = f_2(L_1, L_2, \varphi_2, \beta_3, Z_2) \end{cases} \\ \text{Subject to} \quad 50\,\text{mm} \le L_1 \le 55\,\text{mm} \\ \qquad\qquad 0\,\text{mm} \le L_2 \le 5\,\text{mm} \\ \qquad\qquad 60^{\circ} \le \varphi_2 \le 75^{\circ} \\ \qquad\qquad 12^{\circ} \le \beta_3 \le 20^{\circ} \\ \qquad\qquad 8 \le Z_2 \le 11 \end{cases} \tag{11}$$

4 Result and discussion

4.1 Pareto front

The Pareto front was obtained by NSGA-II with 100 populations and 2000 iterations (as shown in Fig. 8). There is no superior solution in the Pareto front, so the optimal solution must be selected from it. And we selected three optimized cases, marked by A, B, and C in Fig. 8. where A is the optimal head case, which has a higher head than other cases. B is the optimal C_{MEI} case, and the C_{MEI} of this case is lower than that of other cases (which means that the MEI is higher than that of other cases). C is a balanced case between A and B with C_{MEI} and H_d playing equal roles. To verify the accuracy of BPNN and study the flow states of the pump, CFD calculations were carried out on the A, B, and C models. Table 6 shows the geometrical data and performance data of cases from BPNN and CFD.

According to Table 6, it can be found that the head deviation between BPNN and CFD is less than 0.3%, and the deviation of C_{MEI} is less than 1.5%, indicating that BPNN is suitable for pump performance prediction. Compared with the original case, the head of case A is improved by 3.94%, and the C_{MEI} is decreased by 0.99%; the head of case B is improved by 3.23%, and the C_{MEI} is reduced by 1.51%; the head of case C is increased by 3.74%, and the C_{MEI} decreases by 1.17%.

By comparing the difference among cases, some relationships between geometry and performance were found. The axial length L_1 of Case A, B and C are all longer than that of the original case, it indicates longer L_1 helps improve pump head and efficiency simultaneously. As to the trailing edge position of vane L_2, a short L_2 leads to a higher head, and a longer L_2 helps improve efficiency. The vane wrap angle φ_2 has the same effect as L_1 and a relatively small φ_2 benefits improvement of the head. In this optimization, choosing 9 vanes is best for pump performance.

H_d and C_{MEI} of cases A, B, and C are all better than those of the original case, while H_d and η_{PL} were greatly improved. The improvement of η_{PL} is the main cause for the improvement of C_{MEI}. Although the head of case B is lower than that of case A and C, the efficiency of case B under all conditions is higher than case A and C. We believe that the performance of case B is more in line with the demand. Therefore, case B was selected as the optimized model to study the characteristics of unstable flow and the mechanism of energy loss in the pump.

Table 6 Geometry and performance of cases from BPNN and CFD

Parameter	Original case	Case A	Case B	Case C
L_1/(mm)	52	55	54.6	55
L_2/(mm)	2.5	0.7	2.7	2.1
φ_2/(°)	60.5	69.6	71.3	69.7
β_3/(°)	15	12	12	12
Z_2	10	9	9	9
BPNN				
H_d/(m)	45.51	47.42	46.85	47.27
C_{MEI}	122.90	122.87	121.92	122.11
CFD				
H_d/(m)	45.51	47.31	46.98	47.21
C_{MEI}	124.58	123.34	122.69	123.12
η_{PL}/(%)	72.52	73.52	74.16	73.74
η_{BEP}/(%)	77.62	78.49	78.83	78.62
η_{OL}/(%)	76.92	77.15	77.61	77.27
Rel. error				
ε_H/(%)	0.23	0.24	0.29	0.1
ε_{MEI}/(%)	1.37	0.38	0.64	0.82

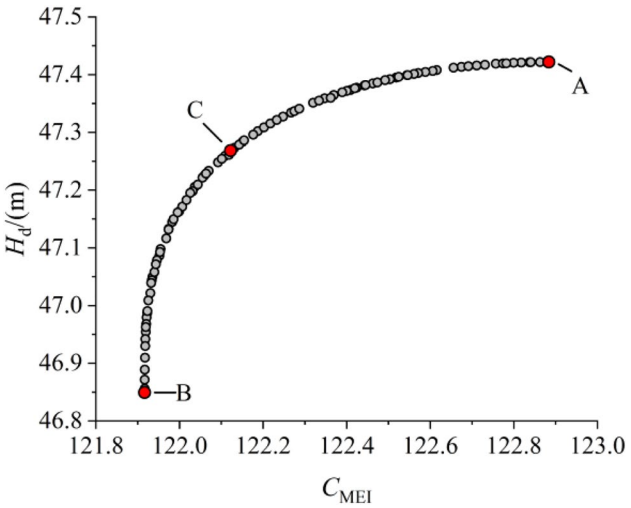

Fig. 8 Pareto front of C_{MEI} and H

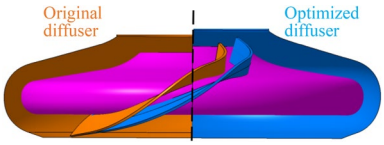

Fig. 9 Diffuser model of the original case and optimized case

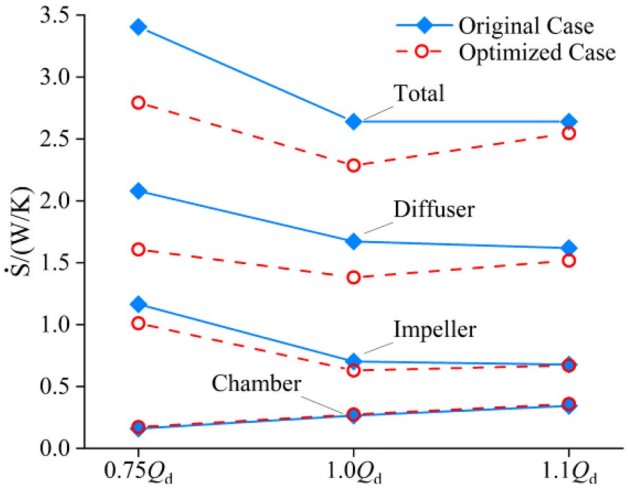

Fig. 10 Local and total entropy production of the original case and optimized case

4.2 Flow analysis

In summary, the optimization method adopted in this research successfully optimized the multistage centrifugal pump, which increased H_d by 3.23%, η_d by 1.56%, and decreased C_{MEI} by 1.51%. The original diffuser model and the optimized diffuser model are shown in Fig. 9. It can be found that the height of the optimized diffuser is higher than the original diffuser, and the vanes of the optimized case have a bigger wrap angle and a relatively smaller vane angle on average.

To improve the performance of the pump, the unsteady flow and mechanism of energy loss characteristics in the pump are further analyzed. As a fast identification method of energy loss, entropy production theory has the advantage of determining the amount and location of energy loss. And a large number of studies have confirmed that entropy generation theory can well reveal the energy loss characteristics of rotating machinery (Gong et al. 2013; Li et al. 2017; Chang et al. 2019; Zhang et al. 2020).

Figure 10 shows the local entropy production (LEP) and total entropy production (TEP) of components under different flow rates. The LEP curves of the two chambers are very similar and the difference is negligible. The LEP of the optimized impeller is lower than that of the original case at 0.75Q_d and 1.0Q_d, but there is little difference at 1.1Q_d. Under all conditions, the diffusers' LEP in the optimized case is lower than in the original case. At 0.75Q_d, the TEP deviation between the original case and the optimized case is the largest, and the efficiency improvement is the largest. At 1.1Q_d, the TEP deviation is minimal and the efficiency improvement is small.

A pump was designed according to the required performance under the design condition, so the design condition is the most important. Therefore, we studied the energy loss mechanism and unstable flow characteristics of the pump at 1.0Q_d first.

Figure 11 shows the head and LEP of impellers and diffusers at 1.0Q_d. In the optimized case, the head of the impellers is slightly higher than the original case, and the LEP of the impellers is lower compared with the original case. And because the diffuser is an energy-consuming component, head drops in the diffuser (ΔH in Fig. 11 means the head loss in diffusers, and it is negative). As shown in the figure, the optimized diffuser has lower head loss and LEP. As a

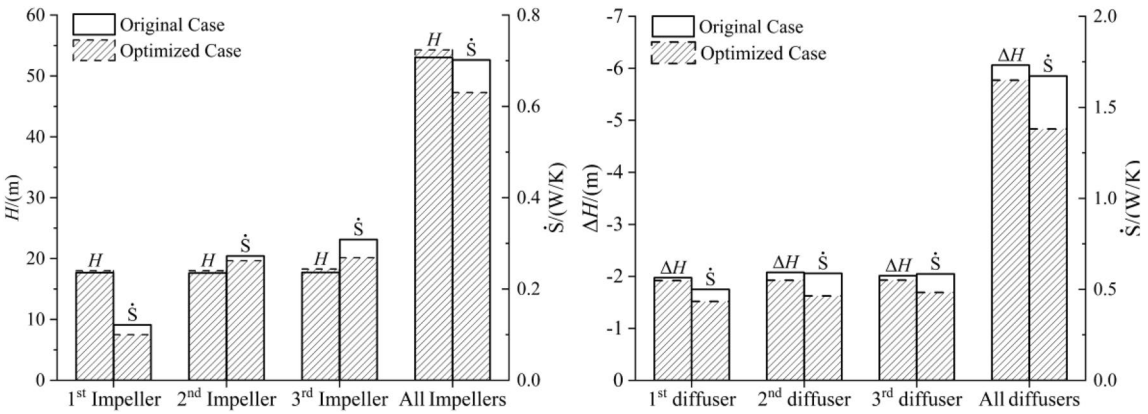

Fig. 11 Head and LEP of impellers and diffusers at 1.0Q_d

result, the performance of the optimized case is better than that of the original case.

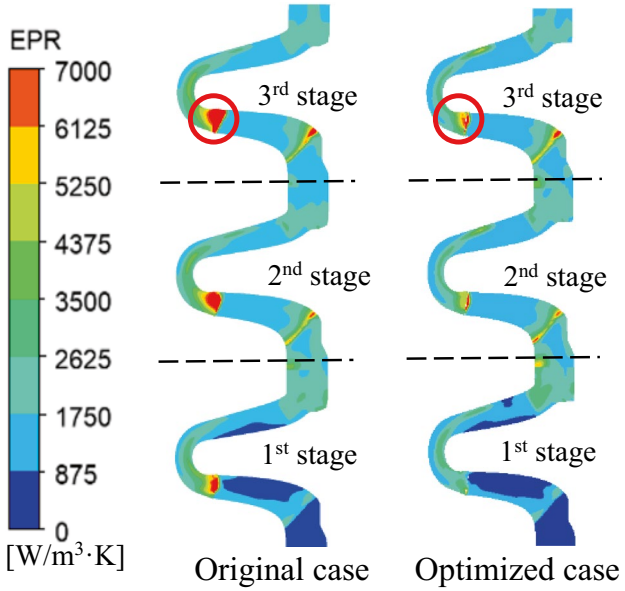

Fig. 12 Average EPR distribution of impellers and diffusers at $1.0Q_d$

To further locate the energy loss in the pump, we analyzed the distribution of the average entropy production rate (EPR) in the meridian surface of impellers and diffusers under the design condition (as shown in Fig. 12). The EPR distribution of the two cases is significantly different at the inlet of diffusers (marked by the red circle), and the energy loss on the interaction surface of impellers and diffusers in the optimized case is greatly reduced. At the same time, the EPR in the diffuser passage of the optimized case is reduced, and the energy loss is improved.

The flow at the interaction surface of the third stage was analyzed (as shown in Fig. 13). On the interaction surface, the flow of fluid in the original case is unstable, and there is a large area of the vortex (marked by the red frame). In this area, the fluid from the impeller impacts the leading edge of the diffuser vane, causing serious flow separation. This situation leads to the occurrence of backflow, which is the main reason for the serious energy loss on the interaction surface. By reducing the inlet angle β_3, the flow of the optimized case on the interaction surface is significantly improved, and there is no obvious flow separation and backflow phenomenon. The smaller inlet angle β_3 weakens the impact of fluid on the leading edge

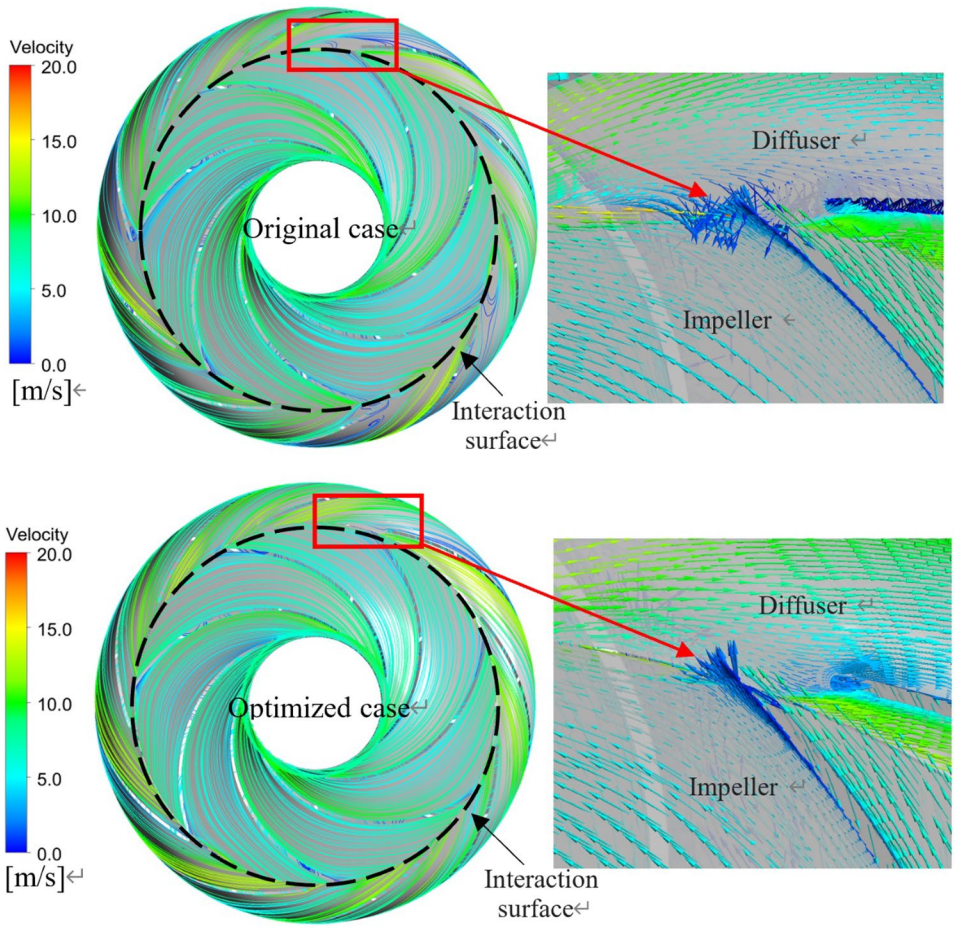

Fig. 13 Streamlines distribution and flow in the third stage of the pump at 1.0 Q_d

of diffuser vanes and makes the fluid enter the diffuser more smoothly.

Figure 14 shows the velocity and vector distribution of the second diffuser at $1.0Q_d$. The velocity gradient in the diffuser of the original case is relatively large. At the suction surface of the vanes, a major backflow problem develops. The diffuser vane of the original case has a larger inlet angle which makes the velocity of the fluid drop faster after entering the diffuser, resulting in more loss during energy conversion. In the optimized case, the velocity gradient is small, the velocity changes smoothly, and the backflow is weakened. It shows that a longer vane length and larger wrap angle φ_2 can prolong the energy conversion process, make the energy conversion process gentler, reduce the energy loss and improve the performance of the pump.

Figure 15 shows the relative pressure (RP) distribution of the second stage in the blade-to-blade view at $1.0Q_d$ ($RP = P - P_0$, P is static pressure, P_0 is average static pressure of the last diffuser outlet). The pressure distribution in the impeller of the original case and optimized case are the same. The pressure distribution at the leading edge of diffusers still maintains a relatively high consistency, but the difference begins to appear in the middle of diffusers. The area of the high pressure in the optimized case is significantly

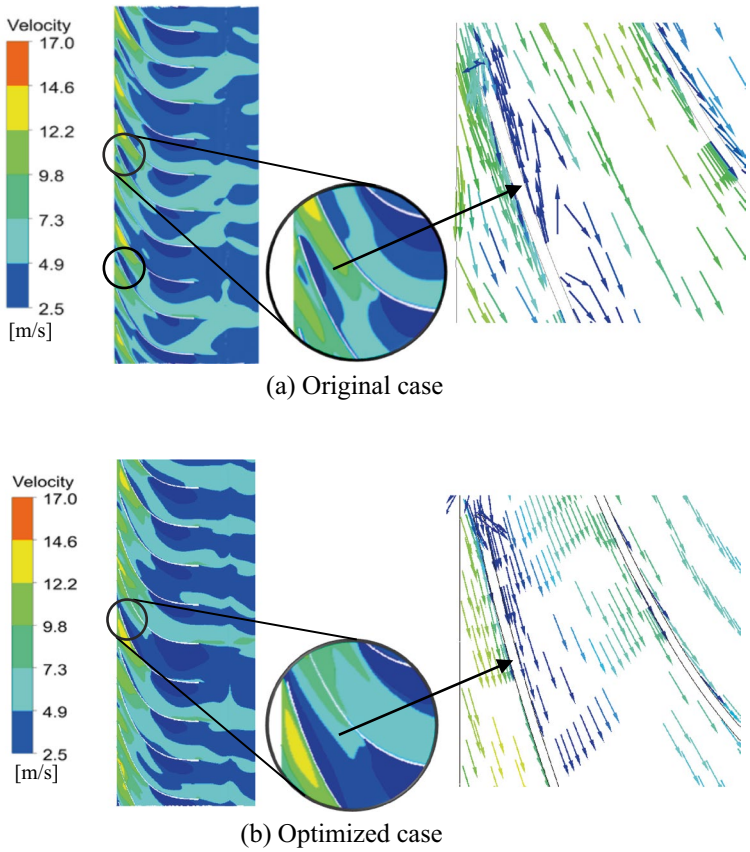

Fig. 14 Velocity distribution and flow of the second diffuser at 1.0 Q_d

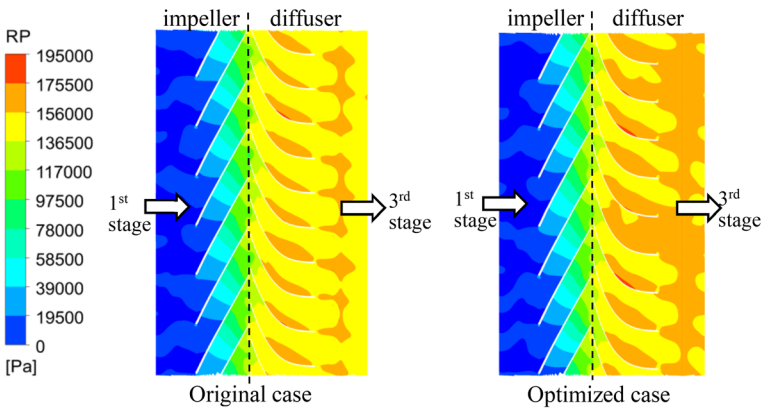

Fig. 15 Pressure distribution of the second stage at 1.0 Q_d

larger than that of the original case. This proves that the optimized diffuser has a stronger ability to convert dynamic energy to static energy, which helps to improve the performance of the pump.

In practical applications, multistage centrifugal pumps operate under off-design conditions frequently. Therefore, it is also important to improve the performance of the pump under off-design conditions. As shown in Table 6, the efficiency of the pump under off-design conditions has also been greatly improved. To comprehensively explore the mechanism of performance improvement for the optimized model, the flow in the pump under the off-design conditions has been analyzed.

Figure 16 shows the average EPR distribution in the meridian surface of impellers and diffusers under off-design conditions. At $0.75Q_d$, a large energy loss was observed at the diffuser's inlet in two cases. The energy loss inside diffusers of the optimized case is significantly improved compared with the original case. At $1.1Q_d$, it is little difference in the EPR distribution between the two cases.

Figure 17 shows the vorticity distribution in the meridian surface of the second diffuser under off-design conditions. By comparing the vorticity distribution under different conditions, it can be found that the high vorticity area at the inlet of the diffuser becomes smaller with the flow rate rising, but there is no improvement inside the diffuser channel.

At $0.75Q_d$, there are a lot of vortices at the inlet of the original diffuser (as pointed out by the arrow). The optimized diffuser reduced the high-vorticity area and improved the energy loss by reducing the inlet angle β_3 to weaken the impact of fluid on the leading edge of the diffuser. Although the high-vorticity area in each channel of the optimized case is not less than that of the original case, it has a wider channel that allows more fluid to pass through. Thus, the optimized diffuser has a better performance at $0.75Q_d$. As shown in Fig. 17, the vorticity distribution at the inlet of the two

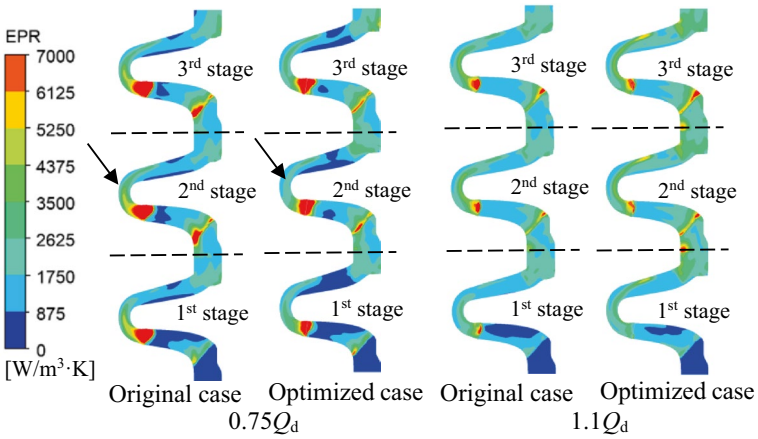

Fig. 16 Average EPR distribution of impellers and diffusers under off-design conditions

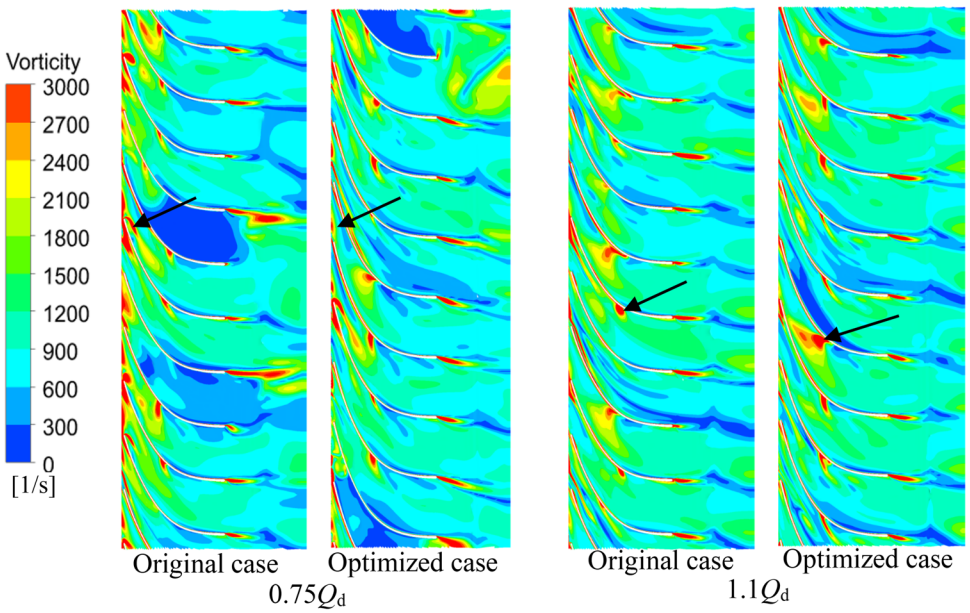

Fig. 17 Vorticity distribution of the second diffuser under off-design conditions

cases is similar at $1.1Q_d$. Although the optimized diffuser has a wider channel, there is more high-vorticity area (as pointed out by the arrow), and the flow passing ability of the diffuser was not well improved. So, the improvement of pump performance at 1.1 Q_d is not obvious.

As discussed above, the optimized case weakens the flow impact on the leading edge of diffuser vanes by reducing the inlet angle β_3 and stabilizes the flow at the inlet of diffusers. By increasing axial length L_1 and wrap angle φ_2, the ability of the diffuser to convert dynamic energy into static energy is enhanced, and the flow inside the diffusers is improved. By reducing the number of blades, the flow passing capacity in the diffusers is enhanced under part load conditions, and the flow is smoother at the outlet of the diffusers.

5 Conclusion

In this research, a multi-objective optimization method combining BPNN and NSGA-II was used to optimize the diffuser of a multi-stage centrifugal pump. The following conclusions were drawn:

(1) The multi-objective optimization method combining BPNN and NSGA-II successfully optimized the performance of the pump under different flow rate conditions. The head at $1.0Q_d$ of the pump was increased by 1.47 m, the C_{MEI} was decreased by 1.89, and the efficiency at $0.75Q_d$, $1.0Q_d$, and $1.1Q_d$ was increased by 1.64%, 1.21%, and 0.69%, the respectively.

(2) The unstable flow characteristics and energy loss distribution of the original case and optimized case are analyzed. At $1.0Q_d$, the impellers' head of the optimized case is 2.37% higher than that of the original case, and the LEP is reduced by 10.17%. The head loss of diffusers is decreased by 4.78%, and LEP is decreased by 17.37%. A smaller inlet angle of the diffuser vane can weaken the flow impact on the leading edge and reduce the energy loss at the inlet of diffusers. A larger axial length and wrap angle can improve the energy conversion ability of diffusers and reduce the energy loss inside diffusers. Reducing the number of vanes can improve the flow passing capacity of the diffusers at small flow rates.

(3) The multi-objective optimization method adopted in this paper is suitable for the optimization design of diffusers. It can provide a new optimization method for diffusers of multistage centrifugal pumps. However, the adaptability of this method for the other hydraulic components (e.g., pump casing, impeller, inducer, etc.) needs further investigation, and in this multi-objective optimization method, how to optimize diffuser and impeller simultaneously can be further extended.

Acknowledgements This research was financially supported by the Natural Science Foundation of Zhejiang Province (No. LGG21E090002, LY21E060004), the China Postdoctoral Science Foundation (No. 2021M691383), the National Natural Science Foundation of China (No. 51779226), and Key Research Plan of Zhejiang Province (No. 2021C01052).

Declarations

Conflict of interest The authors declare that there are no conflicts of interest.

Replication of results The numerical simulation data for the replication of results are provided as supplementary material.

References

Blazek J (2015) Computational fluid dynamics: principles and applications, 3rd edn. Butterworth-Heinemann, Amsterdam

Carravetta A, Fecarotta O, Conte MC (2017) Minimum efficiency Index: testing its performance. World Pumps 2017:34–37. https://doi.org/10.1016/S0262-1762(17)30141-4

Chang H, Shi W, Li W, Liu J (2019) Energy loss analysis of novel self-priming pump based on the entropy production theory. J Therm Sci 28:306–318. https://doi.org/10.1007/s11630-018-1057-5

Cui Y, Geng Z, Zhu Q, Han Y (2017) Review: Multi-objective optimization methods and application in energy saving. Energy 125:681–704. https://doi.org/10.1016/j.energy.2017.02.174

Deb K, Pratap A, Agarwal S, Meyarivan T (2002) A fast and elitist multiobjective genetic algorithm: NSGA-II. IEEE Trans Evol Comput 6:182–197. https://doi.org/10.1109/4235.996017

Derakhshan S, Bashiri M (2018) Investigation of an efficient shape optimization procedure for centrifugal pump impeller using eagle strategy algorithm and ANN (case study: slurry flow). Struct Multidisc Optim 58:459–473. https://doi.org/10.1007/s00158-018-1897-3

Goel T, Dorney DJ, Haftka RT, Shyy W (2008) Improving the hydrodynamic performance of diffuser vanes via shape optimization. Comput Fluids 37:705–723. https://doi.org/10.1016/j.compfluid.2007.10.002

Gong R, Wang H, Chen L, Li D, Zhang H, Wei X (2013) Application of entropy production theory to hydro-turbine hydraulic analysis. Sci China Technol Sci 56:1636–1643. https://doi.org/10.1007/s11431-013-5229-y

Guleren K (2018) Automatic optimization of a centrifugal pump based on impeller–diffuser interaction. Proc Inst Mech Eng A 232:1004–1018. https://doi.org/10.1177/0957650918766688

Han X, Kang Y, Sheng J, Hu Y, Zhao W (2020) Centrifugal pump impeller and volute shape optimization via combined NUMECA, genetic algorithm, and back propagation neural network. Struct Multidisc Optim 61:381–409. https://doi.org/10.1007/s00158-019-02367-8

Li D, Wang H, Qin Y, Han L, Wei X, Qin D (2017) Entropy production analysis of hysteresis characteristic of a pump-turbine model. Energy Convers Manag 149:175–191. https://doi.org/10.1016/j.enconman.2017.07.024

Liu Y, Yang G, Xu Y, Peng F, Wang L (2020) Effect of space diffuser on flow characteristics of a centrifugal pump by computational fluid dynamic analysis. PLoS ONE 15:0228051. https://doi.org/10.1371/journal.pone.0228051

Long Y, Zhu R, Wang D, Yin J, Li T (2016) Numerical and experimental investigation on the diffuser optimization of a reactor

coolant pump with orthogonal test approach. J Mech Sci Technol 30:4941–4948. https://doi.org/10.1007/s12206-016-1014-8
Mckay MD, Beckman RJ, Conover WJ (2000) A Comparison of three methods for selecting values of input variables in the analysis of output from a computer code. Technometrics 42:55–61. https://doi.org/10.1080/00401706.2000.10485979
Meireles MRG, Almeida PEM, Simoes MG (2003) A comprehensive review for industrial applicability of artificial neural networks. IEEE Trans Ind Electron 50:585–601. https://doi.org/10.1109/TIE.2003.812470
Parikh T, Mansour M, Thévenin D (2021) Maximizing the performance of pump inducers using CFD-based multi-objective optimization. Struct Multidisc Optim 65:9. https://doi.org/10.1007/s00158-021-03108-6
Pei J, Gan X, Wang W, Yuan S, Tang Y (2019a) Multi-objective shape optimization on the inlet pipe of a vertical inline pump. J Fluids Eng 141(6):061108. https://doi.org/10.1115/1.4043056
Pei J, Wang W, Osman MK, Gan X (2019b) Multiparameter optimization for the nonlinear performance improvement of centrifugal pumps using a multilayer neural network. J Mech Sci Technol 33:2681–2691. https://doi.org/10.1007/s12206-019-0516-6
Pei Y, Liu Q, Wang G, Song W (2020) Collaborative design of the wrap angles between impeller and space diffuser of diagonal-flow pump. Arab J Sci Eng 45:7835–7849. https://doi.org/10.1007/s13369-020-04725-x
Ren Y, Zhu Z, Wu D, Li X (2018) Influence of guide ring on energy loss in a multistage centrifugal pump. J Fluids Eng. https://doi.org/10.1115/1.4041876
Roache PJ (1994) Perspective: a method for uniform reporting of grid refinement studies. J Fluid Eng 116:405–413. https://doi.org/10.1115/1.2910291
Roache PJ (1997) Quantification of uncertainty in computational fluid dynamics. Annu Rev Fluid Mech 29:123–160. https://doi.org/10.1146/annurev.fluid.29.1.123
Sathish K, Abilash S, Balaji S, Aroon Daniel S, Dhatchinamoorthi V (2021) A review on performance analysis of centrifugal pump impeller. Int J Res Eng Sci Manag 4:44–48
Sayyaadi H, Babaelahi M (2011) Multi-objective optimization of a joule cycle for re-liquefaction of the Liquefied Natural Gas. Appl Energy 88:3012–3021. https://doi.org/10.1016/j.apenergy.2011.03.041
Si Q, Yuan S, Yuan J, Wang C, Lu W (2013) Multiobjective optimization of low-specific-speed multistage pumps by using matrix analysis and CFD Method. J Appl Math 2013:136195. https://doi.org/10.1155/2013/136195
Stel H, Sirino T, Ponce FJ, Chiva S, Morales REM (2015) Numerical investigation of the flow in a multistage electric submersible pump. J Pet Sci Eng 136:41–54. https://doi.org/10.1016/j.petrol.2015.10.038
Wang W, Yuan S, Pei J, Zhang J (2017) Optimization of the diffuser in a centrifugal pump by combining response surface method with multi-island genetic algorithm. Proc Inst Mech Eng E 231:191–201. https://doi.org/10.1177/0954408915586310
Wei Q, Sun X, Asaad YS, Li C (2020) Impacts of blade inlet angle of diffuser on the performance of a submersible pump. Proc Inst Mech Eng E 234:613–623. https://doi.org/10.1177/0954408920935325
Wilcox DC (2006) Turbulence modeling for CFD, 3rd edn. DCW Industries, La Cãnada
Wu T, Wu D, Zhang T, Huang H, Wu Y, Mou J (2021) Influence of diffuser vane number on energy loss of multistage centrifugal pump. Int J Fluid Mach Syst 14:373–382. https://doi.org/10.5293/IJFMS.2021.14.4.373
Yang S, Kong F, Chen B (2011) Research on pump volute design method using CFD. Int J Rotating Mach 2011:137860. https://doi.org/10.1155/2011/137860
Yang Y, Zhou L, Hang J, Du D, Shi W, He Z (2021) Energy characteristics and optimal design of diffuser meridian in an electrical submersible pump. Renew Energ 167:718–727. https://doi.org/10.1016/j.renene.2020.11.143
Zhang F, Appiah D, Hong F, Zhang J, Yuan S, Adu-Poku KA, Wei X (2020) Energy loss evaluation in a side channel pump under different wrapping angles using entropy production method. Int Commun Heat Mass Transf 113:104526. https://doi.org/10.1016/j.icheatmasstransfer.2020.104526
Zhou L, Shi W, Lu W, Hu B, Wu S (2012) Numerical investigations and performance experiments of a deep-well centrifugal pump with different diffusers. J Fluids Eng. https://doi.org/10.1115/1.4006676
Zhou L, Yang Y, Shi W, Lu W, Ye D (2016) Influence of outlet edge position of diffuser vane on performance of deep-well centrifugal pump. J Drain Irrih Mach Eng 34:1028–1034. https://doi.org/10.3969/j.issn.1674-8530.16.0232